Genome context influences evolutionary flexibility of nearly identical type III effectors in two phytopathogenic Pseudomonads

David A. Baltrus[1,2,#]

Qian Feng[3]

Brian H Kvitko[4]

[1]School of Plant Sciences, University of Arizona, Tucson AZ , USA

[2]School of Animal and Comparative Biomedical Sciences, University of Arizona, Tucson AZ , USA

[3]Institute of Plant Breeding, Genetics and Genomics, University of Georgia, Athens GA, USA

[4]Department of Plant Pathology, University of Georgia, Athens GA, USA

#David Baltrus

The University of Arizona

School of Plant Sciences

P.O. Box 210036

Forbes Building, 303

Tucson, Arizona 85721-0036

baltrus@email.arizona.edu

Brian Kvitko

University of Georgia

Department of Plant Pathology

3303 Miller Plant Sciences

Athens, GA 30602

bkvitko@uga.edu

33

Abstract

35

36   Integrative Conjugative Elements (ICEs) are replicons that can insert and excise from chromosomal locations in a site specific manner, can conjugate across strains, and which often carry a variety of genes useful for bacterial growth and survival under specific conditions. Although ICEs have been identified and vetted within certain clades of the agricultural pathogen *Pseudomonas syringae,* the impact of ICE carriage and transfer across the entire *P. syringae* species complex remains underexplored. Here we identify and vet an ICE (PmaICE-DQ) from *P. syringae* pv. maculicola ES4326, a strain commonly used for laboratory virulence experiments, demonstrate that this element can excise and conjugate across strains, and contains loci encoding multiple type III effector proteins. Moreover, genome context suggests that another ICE (PmaICE-AOAB) is highly similar in comparison with and found immediately adjacent to PmaICE-DQ within the chromosome of strain ES4326, and also contains multiple type III effectors. Lastly, we present passage data from *in planta* experiments that suggests that genomic plasticity associated with ICEs may enable strains to more rapidly lose type III effectors that trigger R-gene mediated resistance in comparison to strains where nearly isogenic effectors are not present in ICEs. Taken together, our study sheds light on a set of ICE elements from *P. syringae* pv. maculicola ES4326 and highlights how genomic context may lead to different evolutionary dynamics for shared virulence genes between strains.

53
54

55

56 **Introduction**

57

58   Genome fluidity is crucial for survival of bacterial phytopathogens, as selection

59 pressures on the presence and function of specific virulence genes can dramatically change from

60 host to host (Dillon et al., 2019a; de Vries et al., 2020). Much research characterizing gene

61 composition of bacterial pathogens focuses on presence and absence of specific virulence genes,

62 and therefore often extrapolates from lists of loci to predict virulence and evolutionary potential

63 (Baltrus et al., 2011; Dillon et al., 2019b). However, even if virulence genes are conserved across

64 strains of a particular pathogen, differences in genomic flexibility for shared virulence genes

65 could potentiate different evolutionary outcomes between strains under conditions of strong

66 selection. Here we characterize one instance where such differences in genomic context and

67 fluidity for a set of type III effectors affects evolutionary potential for *Pseudomonas syringae*, and

68 we speculate about the ability of such systems to shift evolutionary dynamics for

69 phytopathogens moving forward.

70

71   Integrative Conjugative Elements (ICEs) are mobile replicons that blend characteristics

72 of both plasmids and prophage and are well known for their ability to harbor antibiotic

73 resistance genes and other niche-association traits across bacteria (Johnson and Grossman,

74 2015). Like conjugative plasmids, ICEs contain all genes and pathways required for conjugation

75 between bacterial cells. Like prophage, ICEs contain site specific recombinases that enable

76 recombination into chromosomal locations and repress the genes responsible for conjugation

77 and replication while in this quiescent state. Most importantly, ICEs also contain cargo regions

78 that can house genes and pathways that directly contribute to dramatic changes in bacterial

79 phenotypes (Lovell et al., 2009; Johnson and Grossman, 2015). Not only can these elements

80 modify phenotypes in their current host cells, but the ability of ICEs to transfer throughout

81 populations and across communities through horizontal gene transfer means that cargo genes

82 present on ICEs can rapidly proliferate if they are beneficial. The rise of sequencing technologies

83 enabling closed bacterial genomes has reinforced the importance of mobile elements in genomes

84 and increased awareness of the prevalence of ICEs throughout bacteria.

85

86   The phytopathogen *Pseudomonas syringae* (sensu lato) is a recognized agricultural pest

87 for many crops throughout the world, with numerous strains well established as laboratory

88 systems for understanding virulence of plant pathogens *in vitro* and *in planta (Baltrus et al.,*

89 *2017)*. The presence of a type III secretion system is critical for virulence *in planta* for many

90 strains of this pathogen, and is used to translocate upwards of 40 effectors proteins per strain

91 from the bacterial cytoplasm into plant cells (Dillon et al., 2019a; Laflamme et al., 2020). Once

92 inside the plant cells, effector proteins can disrupt plant immune responses in a variety of ways

93   to promote bacterial growth and infection. The presence of effector proteins can also be

94   monitored by plant immune responses through the action of R-genes, with recognition of

95   effector protein functions leading to an overarching immune reaction termed effector triggered

96   immunity (ETI)) (Collmer et al., 2000; Jones and Dangl, 2006; Jayaraman et al., 2021). Triggering

97   of the ETI response can quickly shut down nascent infections in resistant plant cultivars and has

98   thus formed the basis of future plans to engineer durable crop resistance to infection through

99   genetic modification and selective breeding (Dong and Ronald, 2019; Laflamme et al., 2020).

100 Thus, type III effectors sit at an evolutionary inflection point where they can be highly beneficial

101 for bacterial growth in some host backgrounds and highly detrimental in others.

102   The presence of virulence genes, including type III effectors, on plasmids and

103 consequent movement across strains can dramatically alter trajectories of virulence evolution

104 for *P. syringae* on different host species (Cazorla et al., 2002; Schierstaedt et al., 2019). Plasmids

105 can be lost or modified if effector proteins are recognized by a potential host, which could

106 enable infections to proceed at a population level despite the ETI response (Grant et al., 2006;

107 Bardaji et al., 2019). Plasmids are not the only element within *P. syringae* genomes displaying

108 plasticity, though. For instance, the effector AvrPphB (aka HopAR1) triggers HR in bean plants

109 that contain the R-gene RPS5 (Qi et al., 2014). AvrPphB is found on an genomic island in certain

110 strains of *P. syringae* pathovar phaseolicola, and under selective pressure from ETI responses

111 bacteria with the island excised from the chromosome and maintained independently as an

112 episome rapidly dominate the population (Godfrey et al., 2011; Neale et al., 2018). Excision of

113 the genomic island containing AvrPphB prevents ETI because this Avr gene is downregulated

114 under episomal replication, but enables this gene to be maintained within a population for

115 infection of host plants where it may be beneficial. ICE elements have also been identified and

116 characterized in *P. syringae* pathovar actinidae strains where their presence/absence is one of the

117 most glaring differences between closely related strains and where they contribute to large scale

118 differences in strain metabolism and resistance to antibacterial compounds (Colombi et al., 2017;

119 McCann et al., 2017; Poulter et al., 2018).

120

121   Here we describe how genomic context in a locus encoding an effector protein, HopQ,

122 differentially affects evolutionary flexibility for this genomic island. Recognition of HopQ by

123 the plant R-gene Roq1 triggers ETI in the host plant *Nicotiana benthamiana*, and thus limits

124 growth of strain *P. syringae* pv. tomato DC3000 (*Pto)* in this host (Wei et al., 2007; Schultink et

125 al., 2017). We characterize the genomic context for *hopQ* and other linked virulence genes in

126 both *Pto*DC3000 and another pathogen, *Pseudomonas syringae* pv. maculicola ES4326

127 (*Pma*ES4326). We demonstrate that this and other effectors are differentially present in an ICE

128 element in *Pma*ES4326 but not in *Pto*DC3000, and confirm that recognition of HopQ also limits

129 growth of *Pma*ES4326 in *N. benthamiana*. These differences are somewhat surprising because at a

130 broad scale these regions appear syntenic. We further show how this differential genomic

4

131   context allows for differential genomic plasticity for *hopQ* between these two strains, by

132   demonstrating that passage of strains in *Nicotiana benthamiana* leads *hopQ* to be more readily lost

133   in *Pma*ES4326 than in *Pto*DC3000. Thus, we directly demonstrate how genomic context for

134   homologous virulence genes in two closely related pathogens can contribute to different

135   evolutionary trajectories for these strains.

136

137   **Methods**

138   <u>Bacterial strains and culturing conditions</u>

139   *E. coli* was routinely cultured at 37°C in LB (Lysogeny broth ; per 1 L = 10 g tryptone, 5 g

140   yeast extract, 10 g NaCl, pH 7.5 + with 15 g agar for solidified media). *P. syringae* was routinely

141   cultured at 25°C or 28°C in either LM (LB modified; per 1L = 10.0 g tryptone, 6.0 g yeast extract,

142   2.0 g $K_2HPO_4 \cdot 3H_2O$, 0.6 g NaCl, 0.4 g $MgSO_4 \cdot 7H_2O$, with 18 g agar for solidified media), KB

143   (King's B; per 1 L = 20.0 g proteose peptone 3, 0.4 g $MgSO_4 \cdot 7H_2O$, glycerol 10 mL, 2.0 g

144    $K_2HPO_4 \cdot 3H_2O$, with 18 g agar for solidified media) or KBC (KB amended with boric acid 1.5

145   g/L and cephalexin 80 mg/L). Liquid cultures were incubated with shaking at 200 rpm. Where

146   appropriate, media was augmented at final concentration with rifampicin (Rf) 40-60 µg/mL,

147   gentamicin (Gm) 10 µg/mL, kanamycin (Km) 50 µg/mL, spectinomycin (Sp) 50 µg/mL, and

148   diaminopimelic acid (DAP) 200 µg/mL for liquid media, 400 µg/mL for solid media for the

149   growth of DAP-auxotrophic *E. coli* strains.

150

151   <u>DNA manipulation</u>

152   Plasmid DNA was routinely purified using the GeneJet plasmid miniprep kit (Thermo

153   Fisher). PCR was conducted with Phusion HiFi polymerase (Thermo Fisher). PCR/reaction

154   cleanup and gel extraction were conducted with the Monarch PCR and DNA cleanup kit and

155   Monarch DNA gel extraction kits (NEB). *E. coli* transformation was conducted by either by

156   preparing competent cells using the Mix and Go! *E. coli* transformation kit (Zymo Research) or

157   standard electro-transformation protocols. *Pma*ES4326 strains were transformed with

158   pCPP5372hopQ (Schultink et al., 2017) plasmid DNA via electro-transformation after washing

159   and concentration of overnight liquid cultures with 300 mM sucrose (Choi et al., 2006).

160   Restriction enzymes, T4 ligase, and Gibson Assembly Mastermix were purchased from NEB.

161   Oligonucleotide primers were synthesized by IDT. Commercial molecular biology reagents

162   were used in accordance with their manufacturer's recommendations.

163   To create the site-specific Tn7 3xmCherry labeling vector pURR25DK-3xmcherry,

164   pURR25 (Teal et al., 2006) was first digested with PstI and recircularized with T4 ligase to

165   remove the *nptII* Km[R] marker gene creating pURR25DK. To replace the *gfp* gene in pURR25DK,

166   the 3xmCherry cassette was PCR amplified from pGGC026 (pGGC026 was a gift from Jan

167   Lohmann (Addgene plasmid # 48831 ; http://n2t.net/addgene:48831 ; RRID:Addgene_48831)

168   using primers bko374

169   (5′**ACATCTAGAATTAAAGAGGAGAAATTAAGCATGGTGAGCAAGGGCGAGGAGGA**

170   **TAACATG 3′) and** bko375 (5′

171   **CAGGAGTCCAAGCTCAGCTAATTAAGCTTACTTGTACAACTCATCCATACCACCTGT**

172   **TGA 3′)** to introduce 30 bp 5′ overlaps corresponding to the *gfp* flanking regions. Gibson

173   assembly was used to join the 3xmCherry PCR amplicon with pURR25DK backbone digested

174   with *Bse*RI and partially digested with *Hind*III.

175

176   <u>Bacterial conjugation and creation of mutant strains.</u>

177   Conjugations were performed by mixing 15 µL of 5-fold concentrated, washed,

178   overnight LM liquid cultures of each parent strain and co-culturing at 28°C overnight on sterile

179   nitrocellulose membranes on either LM or LM+DAP plates (for conjugations with DAP-

180   auxotrophic *E. coli* donor strains). Tn7 transposition conjugations always included the *E. coli*

181   RHO3 pTNS3 Tn7 transposase helper strain as a third parent. For all conjugation experiments

182   cultures of each parent strain were included separately as controls. *Pma*ES4326 merodiploid

183   exconjugants of pCPP5729 (pK18msGmΔ*hopQ1)* were recovered on LM Km (Kvitko et al., 2009).

184   Resolved Pma ES4326 pCPP5729 merodiploids were recovered via counter-selection on LM Rf

185   +10% sucrose and sucrose resistant clones were screened for kanamycin sensitivity by patch

186   plating indicating the loss of the pK18ms plasmid backbone (Kvitko and Collmer, 2011).

187   Derivative *att*Tn7-3xmCherry transposant strains were recovered on LM Sp and pink clones

188   were selected after 4 days incubation at 4°C and restreaked to isolation. To test the native

189   mobility of PmaICE-DQ, conjugation was conducted as described above with the *Pma* ES4326

190   pCPP5729 merodiploid as the donor parent and *att*Tn7-3xmCherry derivatives of *Pto* DC3000 *Pma*

191   ES4326 ΔPmaICE-DQ strains (*Pma*ES4326ΔDQ3 and *Pma*ES4326-C-LA-P5-20-1) as recipients.

192   PmaICE-DQ exconjugants were recovered on LM Rf Sp Km. Conjugation frequency was

193   calculated as the number of Sp^{R}Km^R colonies recovered per recipient CFU as determined by

194   dilution plating.

195

196   <u>*Nicotiana benthamiana* growth, inoculation and bacterial passage assays.</u>

197   *Nicotiana benthamiana*, WT LAB accession, and *roq1-1* (Qi et al., 2018) were grown in a Conviron

198   Adaptis growth chamber with 12 h light (125 µmol/m^2/s) at 26°C and 12 h dark at 23°C. Plants

199   were used at 5-7 weeks post germination. To prepare inoculum, *P. syringae* cultures were

200   recovered from fresh KB plate cultures, resuspended in 0.25 mM MgCl$_2$, standardized to OD$_{600}$

201   0.2, and serially diluted 10,000X to ~3x10^4 CFU/mL. Cell suspensions were infiltrated with a

202   blunt syringe into either the 3rd, 4th or 5th leaves. Infiltrated spots were allowed to dry fully

203   and then plants were covered with a humidity dome and kept at 100% humidity for 6-8 days to

204   allow symptoms to develop. At end point, leaves were photographed to document symptoms

205   and four 4 mm leaf punches (~0.5 cm^2 total) were collected with a biopsy punch from each

6

206 infiltrated area. Discs were macerated in 0.1 mL 0.25 mM $MgCl_2$ using an Analytik Jena

207 SpeedMill Plus homogenizer and the bacterial CFU/cm^2 leaf tissue was determined by serial

208 dilution spot planting on LM Rf.

209   For *P. syringae* passaging in *N. benthamiana*, single colonies of *Pto* DC3000 WT and

210 *Pma*ES4326 were inoculated into LM Rf liquid cultures. Samples of the initial cultures (P0) were

211 cryo-preserved at -80C in 15% final strength sterile glycerol. The liquid cultures were diluted

212 1000X in 0.25 mM $MgCl_2$ to approximately 5×10^5 CFU/mL prior to syringe infiltration into three

213 leaf areas establishing 3 lineages (A, B, C) each for Pto DC3000 and Pma ES4326. Tissue samples

214 were collected 6-7 days post inoculation and processed as described above. Bacteria cultured

215 from the 10^{-1} tissue macerate dilutions of each lineage were directly scraped from the dilution

216 plate with an inoculation loop and suspended in 1 mL 0.25 mM $MgCl_2$. These suspensions were

217 then sub-cultured 5 μL into 5 mL LM Rf and diluted as described above to create inoculum for

218 the next passage. This passaging scheme was repeated five times and samples of both the post-

219 passage recovered bacteria (P1) and the corresponding sub-cultured bacteria (P1c) were cryo-

220 preserved for each lineage and each passage. To screen for changes in *N. benthamiana* disease

221 compatibility with passaged strains in a medium-throughput format, bacteria from the P5 cryo-

222 preserved samples were streaked to isolation on KBC plates and isolated "P5" colonies were

223 cultured in 200 μL of LM Rf in sterile 96 well microtiter plates along with Pto DC3000, *Pto*

224 DC3000Δ*hopQ*, *Pma* ES4326 and *Pma*ES4326ΔDQ3 control strains. Cultures were serially-diluted

225 5000X in 0.25 mM $MgCl_2$ to $\sim 3 \times 10^4$ CFU/mL and inoculated into *N. benthamiana* leaves as

226 described. Inoculum concentration was verified via serial dilution spot plating. Inoculated areas

227 were monitored for disease symptoms compared to their respective control strains over the

228 course to 6-8 days and CFU/cm^2 leaf tissue was determined for each strain as described above.

229 Isolated colonies of strains that displayed bacterial load and symptoms comparable to their

230 respective Δ*hopQ* backgrounds were subcultured from the dilution spot count plates and

231 retained.

232

233 <u>Genome sequencing and Assembly</u>

234

235   For each strain with a genome sequence reported herein, a frozen stock was streaked to

236 single colonies on King's B (KB) agar plates, at which point a single colony was picked to 2mL

237 KB liquid and grown overnight on a shaker at 27°C. Genomic DNA was extracted from these

238 overnight cultures using a Promega (Madison, WI) Wizard kit and including the optional

239 RNAse step. Each strain was sequenced using multiple technologies, and in each case

240 independent DNA isolations were used to prepare libraries for different sequencing platforms.

241 Illumina sequencing for strains was performed by MiGS (Pittsburgh, PA) using their standard

242 workflow. As described in (Baym et al., 2015), this workflow uses an Illumina tagmentation kit

243 for library generation, followed by sequencing on a NextSeq 550 instrument with 150-bp paired-

7

244   end reads. Trimmomatic was used for adaptor trimming (Bolger et al., 2014) . For nanopore

245   sequencing for strain *Pma*ES4326-D, a library was prepared from unsheared DNA using the

246   Rapid sequencing kit (SQK-RAD004) and sequenced on a Flongle flowcell. For nanopore

247   sequencing for strains *Pma*ES4326-C,*Pma*ES4326ΔDQ3, and *Pma*ES4326-C-LA-P5-20-1, each

248   library was prepared using unsheared DNA as an input to the LSK109 ligation sequencing kit

249   and was sequenced on R9.4 MinION flowcells. Nucleotide bases were called during sequencing

250   using Guppy v3.2.6 in Fast-Mode. All genomes were assembled using Unicycler v.0.4.8 (Wick et

251   al., 2017). The public facing genomes for *Pma*ES4326-D and *Pma*ES4326-C were annotated using

252   PGAP (Tatusova et al., 2016). Genomes for *Pma*ES4326ΔDQ3, and *Pma*ES4326-C-LA-P5-20-1

253   found in Figshare were annotated using Prokka v 1.14.6 (Seemann, 2014). Default parameters

254   were used for all software unless otherwise specified.

255

256   **Results**

257

258   <u>Complete Genome Sequences for Multiple Isolates of *Pma*ES4326 Highlights Genome Flexibility</u>

259   <u>for this Strain</u>

260

261   We previously reported a draft genome sequence for an isolate of *Pma*ES4326 acquired

262   from the lab of Jeff Dangl (Baltrus et al., 2011), and our first goal was to generate a complete

263   genome sequence for this strain (referred to herein as *Pma*ES4326-D, Table 1). We used MiGS

264   (Pittsburgh, PA) to generate Illumia reads for *Pma*ES4326-D, and their workflow generated a

265   total of 3,284,990 paired reads and 418Mb (~64x coverage) of sequence. We also independently

266   isolated genomic DNA and sequenced using an Oxford Nanopore MinION to generate 32,291

267   reads for a total of 465Mb (~71x coverage) of sequence with a read N50 of 30,656 bp. Assembly

268   of these reads resulted in a complete circular chromosome and four separate plasmids. Notably,

269   our isolate of *Pma*ES4326-D contains three previously reported plasmids (pPma4326A,

270   pPma4326B, pPma4326E) but also appears to have lost two different plasmids (pPma4326C and

271   pPma4326D) first reported as present in this strain by Stavrinides et al., 2004. The assembly for

272   this strain appears to contain an additional ~350kb plasmid that was not reported by Stavrinides

273   et al. and which we name pPma4326F following earlier naming conventions.

274   Given the absence of two plasmids from *Pma*ES4326-D, we sought to generate a genome

275   assembly from a different lab isolate, acquired from the lab of Alan Collmer referred to here as

276   *Pma*ES4326-C (Table 1). We used MiGS (Pittsburgh, PA) to generate Illumia reads for the

277   Collmer lab version of *Pma*ES4326, and their workflow generated a total of 3,757,284 paired

278   reads and 485Mb (~74x coverage) of sequence. We also independently isolated genomic DNA

279   and sequenced using an Oxford Nanopore MinION to generate 55,845 reads for a total of

280   700Mb (~107x coverage) of sequence with a read N50 of 24,669bp. Hybrid assembly of all read

281   types resulted in a single chromosome that appears nearly complete but was not circularized by

282   Unicycler. However, this assembly does contain all predicted circular plasmids as well as
283   pPmaES4326F.
284
285   An ICE Element Hotspot In *Pma*ES4326
286
287   Genomic inspection of the region containing type III effectors *hopQ* and *hopD* in strains
288   *Pma*ES4326-C and *Pma*ES4326-D indicate that this area is a potential hotspot for genomic
289   plasticity. Specifically, in a region bordered by *clpB* and the type III effector *hopR,* gene content
290   characterization strongly suggests the presence of two independent integrative conjugative
291   elements (ICEs, Figure 1). Both ICEs are approximately 70kb in length, and are found adjacent
292   to tRNA loci encoding a proline anticodon. Moreover, roughly 70% of each element is
293   composed of sequences with >95% nucleotide similarity and which encode many of the
294   structural genes predicted to be involved in ICE proliferation and integration. These conserved
295   genes include predicted integrases/recombinases, pilus proteins and ATPases, regulator
296   proteins, a topoisomerase (*topB*) and helicase, chromosome partitioning proteins (*parB*), DNA
297   coupling proteins (*traD*), an NTPase (*traG*), and numerous loci annotated as "integrative
298   conjugative element proteins".
299   Despite relatively high sequence similarity across these two closely related ICEs
300   positioned successively in the genome of *Pma*ES4326, gene comparisons suggest the presence of
301   three distinct cargo regions that clearly differentiate these elements (Figure 1). The first ICE
302   contains type III effector proteins *hopAO* and *hopAB3-1* (*hopPmaL*) in two different predicted
303   cargo regions, and so we name this region *Pma*ICE-ABAO. The second ICE contains loci for
304   type III effectors *hopD* and *hopQ* as well as the lytic transglycosylase *hopAJ1*, and so we name
305   this ICE *Pma*ICE-DQ. Cargo region one contains four predicted ORFs in *Pm*aECE-ABAO and
306   fourteen predicted ORFs in PmaICE-DQ. Cargo region two contains two predicted ORFs in
307   PmaICE-ABAO and seven predicted ORFs in PmaICE-DQ, including the effectors *hopAO*, *hopD*,
308   and *hopQ.* Cargo region three contains 6 predicted ORFs in PmaICE-AO and two in PmaICE-
309   DQ. Aside from the type III effectors, many of loci potentially encoded by these cargo regions
310   are annotated as hypothetical proteins or as parts of IS elements and transposons.
311
312   Differential contexts for the genomic island containing *hopD* and *hopQ* across *Pma*ES4326 and
313   *Pto*DC3000
314
315   The type III effectors HopD and HopQ are nearly sequence identical in two
316   phytopathogens commonly used as laboratory models for studying *P. syringae* virulence,
317   *Pto*DC3000 and *Pma*ES4326 (Baltrus et al., 2011). Furthermore, these effectors are found in
318   roughly the same genomic context in the two strains, bordered on one side by *clpB* and on the
319   other by the type III effector *hopR* (Figures 1 and 2). Broad comparisons between *Pto*DC3000 and

320   *Pma*ES4326 further suggest that these effectors form a genomic island along with a third effector

321   (*hopR*) across these two strains (Figure 2), an island which has been referred to as cluster IV in in

322   the *Pto*DC3000 genome (Kvitko et al., 2009). Moreover, the size of the region between *clpB* and

323   *hopR* in *Pto*DC3000 is roughly 70kb, which closely approximates the size of each ICE in

324   *Pma*ES4326. However, while we note above that this region is likely one of high genomic

325   plasticity in *Pma*ES4326, the region containing *hopDQ* in PtoDC3000 lacks many of the

326   hallmarks associated with either PmaICE-DQ or PmaICE-ABAO. While this region for

327   PtoDC3000 does contain subtle hints that suggest the presence of past ICE integration, such as a

328   recombinase syntenic with and similar to those found in the *Pma*ES4326 ICEs, numerous parts

329   of this region in *Pto*DC3000 are quite divergent from that in *Pma*ES4326 (Figure 2). Specifically,

330   numerous ICE-associated proteins appear to be absent from this region in *Pto*DC3000 (Figure 2),

331   and numerous insertion sequence elements and transposase genes have instead proliferated.

332   Such diversity renders accurate evaluation and comparison of evolutionary histories between

333   *Pto*DC3000 and *Pma*ES4326 very challenging at the moment.

334

335   <u>An evictable ICE Containing HopQ and HopD in *Pma*ES4326</u>

336

337   ICEs are categorized by their ability to cleanly excise from the genome, and we

338   confirmed the prediction that the type three effectors *hopQ* and *hopD* are contained in an

339   excisable region in *Pma*ES4326 in two distinct ways. As a first step, we characterized the size of

340   the region excised during intentional creation of a *hopQ-* mutant. To do this, we generated a

341   merodiploid strain in which plasmid pCPP5729 was recombined into a region adjacent to *hopQ*,

342   and then selected for resolution of the merodiploid through plating on sucrose. Presence of *sacB*

343   in plasmid pCPP5729 renders the merodiploid sensitive to killing by sucrose. Notably, this

344   merodiploid also contains regions sequence identical to those surrounding *hopQ* in *Pma*ES4326

345   and so we originally expected that the *hopQ* gene could be locally deleted through RecA-

346   dependent homologous recombination. We isolated sucrose resistant isolates after plating this

347   merodiploid, and identified strains that were neither WT reverants nor clean *hopQ* deletions by

348   PCR genotyping using previously validated primers. We refer to the focal one of these strains

349   hereafter as *Pma*ICEΔDQ3. Interestingly, while no clean *hopQ* deletion mutants were identified

350   after sucrose counter-selection of merodiploid strains, WT revertants were. We then performed

351   whole genome sequencing to confirm whether the PmaICE-DQ genomic region was lost under

352   these selective conditions in *Pma*ICEΔDQ3. As one can see in Fig. 3, *hopQ* and the surrounding

353   regions that are predicted to be part of PmaICE-DQ have been lost in this strain, confirming that

354   this region can be cleanly and completely excised from the chromosome in a manner consistent

355   with the action of site-specific recombinases contained by ICEs. Searches of both the raw

356   Illumina and Nanopore reads for remnants of *hopQ* or *hopD* yielded no hits despite extensive

357 depth (~51x for Illumina reads and ~27x for Nanopore reads), which suggests that PmaICE-DQ
358 was fully lost and not retained as an episome in *Pma*ICEΔDQ3 (data not shown).

359

360 Loss of PmaICE-DQ Enables Virulence of *Pma*ES436 on *N. benthamiana*

361

362   The presence of hopQ in *Pma* would be expected to elicit the ETI response in *Nicotiana*
363 *benthamiana* accesions containing the R-gene Roq1, and a lack of compatible infection and
364 disease. Given this information, we tested whether *Pma*ICEΔDQ3 would gain compatibility
365 with *N. benthamiana*. The ΔPmaICE-DQ strain did in fact gain disease compatibility with *N.*
366 *benthamiana* in a manner similar to the gain-of-compatibility phenotypes previously observed
367 for PtoDC3000 Δ*hopQ1-1* mutants and *Xanthomonas euvesicatoria* 85-10 Δ*xopQ* mutants (Wei et
368 al., 2007; Adlung et al., 2016). Furthermore, *N. benthamiana* incompatibility could be restored in
369 *Pma*ICEΔDQ3 by *hopQ* complementation *in trans* and PmaES4326 incompatibility was not
370 observed in *roq1-1* CRISPR-edited *N. benthamiana* as shown in Fig. 4 (Qi et al., 2018) .

371

372

373 Loss of PmaICE-DQ Under Selection *In Planta*

374

375   Observing that we could readily recover strains containing spontaneous evictions of the
376 PmaICE-DQ under the selective pressure of sucrose counter-selection, and that *Pma*ICEΔDQ3
377 gained disease compatibility with *N. benthamiana,* we tested whether the selective pressure of
378 ETI would also result in recovery of strains with PmaICE-DQ evicted. We inoculated *N.*
379 *benthamiana* with *Pma*ES4236-C and PtoDC3000 at approximately 5x10^5 CFU/mL establishing
380 three lineages for each strain (Lineage A, LA; Lineage B, LB; Lineage C, LC). Six to seven days
381 post inoculation bacteria from each lineage were recovered and used to create new inoculum to
382 passage the bacteria through *N. benthamiana* a total of five times. Twenty-two isolated clones of
383 each passage 5 (P5) lineage were screened for altered *N. benthamiana* disease compatibility
384 phenotypes. For *Pto*DC3000, none of the 66 P5 clones tested produced disease symptoms
385 distinct from the WT *Pto*DC0000 control. However, for *Pma*ES4326, 7 of 66 (2 LA, 3 LB, 2 LC) P5
386 clones were able to cause disease symptoms similar to *Pma*ICEΔDQ3 (See Fig. 5). Genome
387 sequencing of *Pma*ES4326-C clone LA-P5-20-1 confirmed the loss of PmaICE-DQ in this strain
388 identical to that observed in the *Pma*ICEΔDQ3 strain recovered after sucrose counter-selection
389 (Table 2, Figure 3).

390

391 Transfer of PmaICE-DQ Between Strains

392

393   Aside from being able to excise from the genome, ICE elements are also categorized by
394 their ability to transfer across bacterial strains, and we therefore tested whether PmaICE-DQ

395 could undergo conjugation to a naive strain. To do this, the PmaICE-DQ merodiploid described

396 above (the precursor to *Pma*ICEΔDQ3) was co-cultured with either *Pto*DC3000 or two

397 independent PmaΔICE-DQ strains (*Pma*ICEΔDQ3 and *Pma*ES4326-C-LA-P5-20-1). After their

398 initial creation, these recipient strains were labeled with a Tn7 3xmCherry SpR resistant

399 transposon to differentiate them from the donor strain. Conjugations between these strains were

400 then plated on kanamycin and spectinomycin selective media (Fig. 6A). No kanamycin and

401 spectinomycin resistant mCherry exconjugants were recovered from the *Pto*DC3000

402 conjugation. However, we were able to recover kanamycin and spectinomycin resistant

403 mCherry+ exconjugants in *Pma*ES4326ΔICE-DQ strains at rates of 2.50×10^{-7} stdev $\pm 1.23^{-7}$ and

404 3.05×10^{-7} stdev $\pm 1.51^{-7}$ exconjugants per recipient respectively in derivatives of *Pma*ICEΔDQ3and

405 *Pma*ES4326-C-LA-P5-20-1 (Fig. 6B) which strongly suggests that the PmaICE-DQ element is

406 readily transmissible into *Pma*ES4326 strains lacking PmaICE-DQ.

407

408

409 **Discussion**

410

411 Integrative Conjugative Elements (ICEs) are important drivers of evolutionary dynamics

412 within and across bacterial populations and communities because of their potential to

413 disseminate genes and pathways through horizontal transfer (Johnson and Grossman, 2015).

414 Genes encoded by ICEs often impart phenotypes critical for survival under specific

415 environmental conditions, including antibiotic resistance loci as well as phage defense systems

416 (Botelho and Schulenburg, 2021; LeGault et al., 2021). In the phytopathogen *Pseudomonas*

417 *syringae*, plasticity of ICE elements encoding genes involved in heavy metal resistance, type III

418 effectors, and carbon metabolism has been identified as the main difference between epidemic

419 strains causing disease across kiwi orchards in New Zealand and with previous outbreaks

420 (Colombi et al., 2017; McCann et al., 2017; Poulter et al., 2018). Despite the accumulation of

421 numerous complete genomes sequences for *P. syringae* and related species and the likelihood of

422 ICEs to impart traits that affect growth in agricultural settings, to date there have been relatively

423 few ICEs identified and vetted for this pathogen.

424

425 Placement of genes and pathways in ICEs may be especially important under conditions

426 of fluctuating selection pressures where selection pressures on cargo genes in an ICE switch

427 from positive to negative depending on the environment. One such scenario involves the

428 presence of type three effector genes, which are bacterial proteins delivered from symbionts

429 into eukaryotic host cells and which are critical for pathogenesis of *P. syringae* strains *in planta*

430 *(Grant et al., 2006)*. Type three effectors are particularly well studied in phytopathogens such as

431 *Pseudomonas syringae*, where they can be of exceptional benefit on some host plants by enabling

432 strains to overcome host immune responses but may also directly trigger immune responses

433   based on the presence of cognate immune receptors on other host genotypes (Dillon et al.,

434   2019a; Laflamme et al., 2020). The presence of type three effectors on ICEs would enable the

435   rapid transmission of these critical virulence genes across strains, while also enabling genes to

436   be rapidly lost from lineages if host genotypes shift such that the effectors are recognized by R

437   gene pathways. Extending this thought, effectors in ICEs that are recognized by hosts are

438   potentially lost more readily through ICE element excision than through mutation (given

439   dedicated excision machinery of the ICEs), which may facilitate adaptation if a strain

440   encounters a resistant host background. While not an extensive experiment, our passage

441   experiment where a subset of *Pma*ES4326 but not *Pto*DC3000 clones becomes compatible with

442   *N. benthamiana* does demonstrate that parameter space exists for such a scenario. Moreover,

443   effectors that are inactivated through mutation can only be reactivated by reversion mutations

444   or through horizontal transfer and acquisition from different strains. In contrast, if effectors are

445   found on ICEs and lost through excision, it's possible that a small resident pool of strains

446   containing these ICES will remain on other host plants or throughout the environment,

447   facilitating rapid reacquisition of effectors that could be beneficial under different contexts.

448   Lastly, there are a plethora of type III effectors in *P. syringae* that carry out a variety of functions

449   across different host plants and resistance backgrounds (Dillon et al., 2019a). Some of these

450   effectors can be considered "core" and found in syntenic locations across strains while others

451   are more variably present. It's possible that presence of effectors in ICEs could itself reflect

452   something about the characteristics of these effectors, in that the proteins found as cargo on

453   ICEs may be subject to higher levels of fluctuating selection across hosts than those found in the

454   core set.

455

456   HopQ and HopD are often found together on genomic islands in *P. syringae* genomes,

457   and have been associated with adaptation to agriculturally important crop plants (Wei et al.,

458   2007; Baltrus et al., 2011; Monteil et al., 2016). Presence of *hopQ* in an ICE in strain *Pma*ES4326

459   sets up an interesting scenario because a nearly identical version of this effector is present in a

460   somewhat syntenic position in a relatively closely related strain *Pto*DC3000 except that this

461   effector is not part of an intact ICE. Therefore, this genomic context suggests that *hopQ* would

462   experience more evolutionary flexibility in *Pma*ES4326 than in *Pto*DC3000 due to its presence in

463   an ICE. To test for differences in evolutionary flexibility, we passaged replicate populations of

464   both *Pma*ES4326 and *Pto*DC3000 in a cultivar of *Nicotiana benthamiana* which can recognize and

465   mount an immune response to HopQ. As such, wild type versions of *Pma*ES4326 and

466   *Pto*DC3000 are recognized by this cultivar and trigger an immune response which prevents

467   disease. However, we found that passage of *Pma*ES4326 (but not *Pto*DC3000) from plant to plant

468   rapidly selected for cells of *Pma*ES4326 that didn't trigger the immune response. Therefore,

469   presence of this type III effector inside of an ICE enables rapid loss of the recognized effector

13

470 under conditions of negative selection and there is much less flexibility in this loss in a strain
471 where the effector is not present in an ICE.
472
473   One other curious feature of the genome of *Pma*ES4326 is that it encodes two distinct but
474 highly similar ICE elements (Figure 1). The configuration is particularly interesting as two
475 distinct ICE elements have integrated successively into the *Pma*ES4326 genome and many of the
476 genes involved in ICE functions are quite conserved between the two. It also appears as though
477 integration of the first element recreated a tRNA with a proline anticodon and that the second
478 ICE element can use this as a further integration point. Indeed, excision of PmaICE-DQ in both
479 strains reported here also deletes one of the predicted proline tRNAs. It may therefore be no
480 coincidence that two ICE elements that are highly similar (but which contain different cargo
481 regions) can integrate successively into the genome as it's straightforward to imagine that
482 highly specific recombinases would have similar target sequences.
483
484   Although not the main focus of this manuscript, we also report on plasticity of the
485 *Pma*ES4326 genome writ large across lab derived strains (Table 2). As the number of complete *P.*
486 *syringae* genome sequences accumulates, it is becoming more apparent that strain *Pma*ES4326 is
487 notable compared to the rest of the species complex because it contains so many secondary
488 replicons as well as additional elements that contribute to genomic plasticity (Stavrinides and
489 Guttman, 2004; Stavrinides et al., 2012). Notably, many of these plasmids appear to contain
490 genes involved in virulence and so acquisition of these replicons through horizontal gene
491 transfer has likely contributed to the pathogenic ability of this strain across multiple hosts.
492 However, there is a clear downside to the large plasmid repertoire of *Pma*ES4326 as
493 demonstrated by genome sequences reported here. Although we can't definitively catalogue
494 passage histories, genome sequences from isolates from the Dangl and Collmer labs are likely
495 not diverged by >10 passages total. In this time, the Dangl isolate (*Pma*ES4326-D) has lost two
496 different plasmids that were originally reported by Stavrinides et al. and which are contained in
497 the Collmer lab isolate (*Pma*ES4326-C). Indeed, genome assemblies for the PmaICE-DQ excision
498 strain suggest that this strain has also lost at least one plasmid in addition to the PmaICE-DQ
499 after only 3 additional passages in culture. Lastly, even though this strain was extensively
500 surveyed for plasmids through gel electrophoresis and Sanger sequencing, we report the
501 existence of an additional large plasmid present within all sequenced isolates of this strain.
502
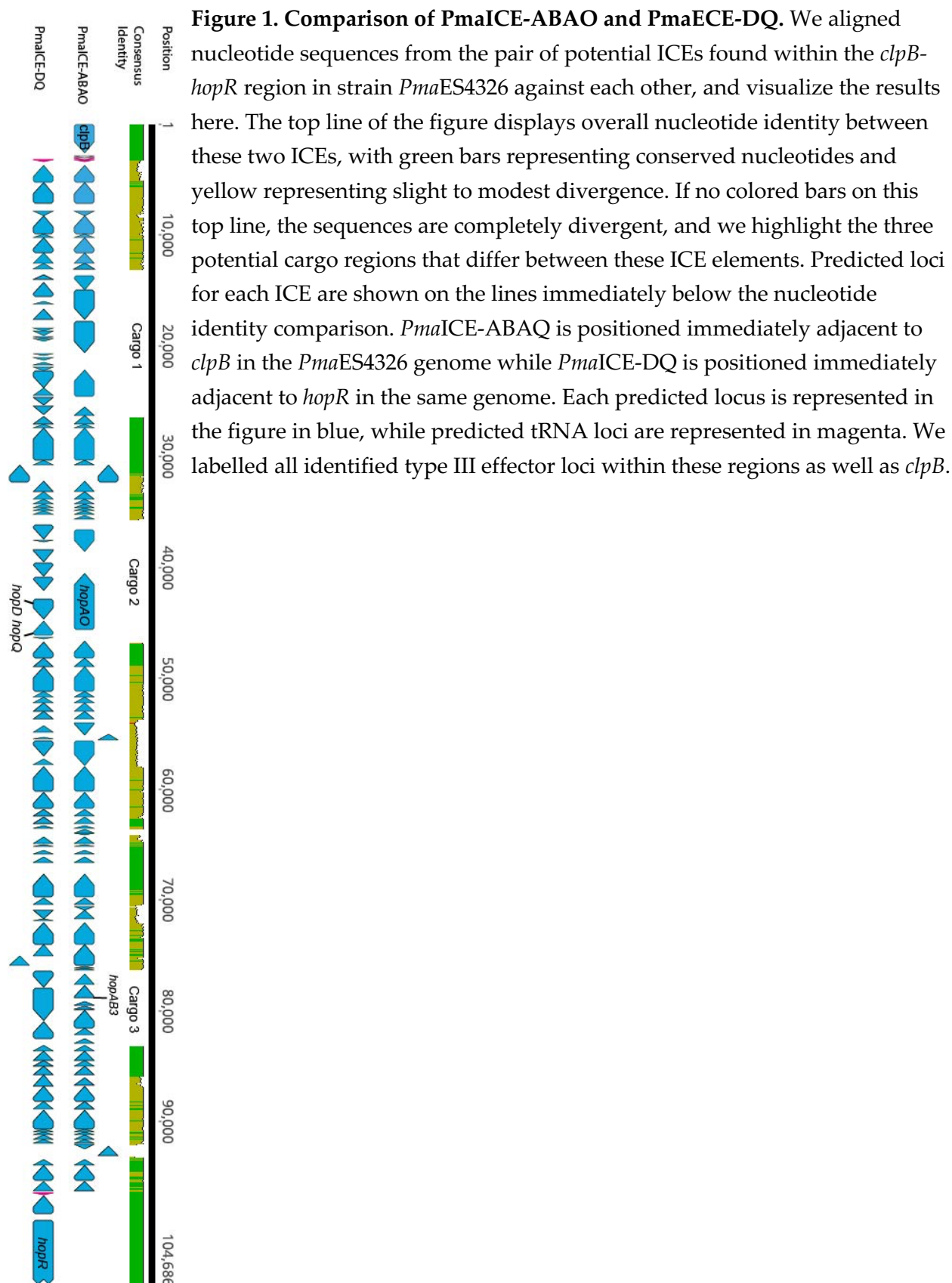503 **Data Availability**
504
505   Sequencing reads for each of the genomes have been posted in the SRA at accessions
506 listed in Table 1. Genome assemblies for each genome have been posted at either Genbank or
507 Figshare and are listed in Table 2.

508

509 **Acknowledgments**

510

516

517

Table 1: Sequencing of *Pma*ES4326 Strains

Strain	Reads (Illumina/Nanopore)	Total bp Sequenced Mb (Illumina/Nanopore)	Read N50 Nanopore bp	Total Sequencing Depth (Illumina/Nanopore)	SRA Accession (Illumina/Nanopore)
*Pma*ES4326-D	3,284,990 / 32,291	418.372 / 465.212	30,656	64x / 71x	SRR15988725 / SRR15988724
*Pma*ES4326-C	3,757,284 / 55,845	485.469 / 700.483	23,669	74x / 107x	SRR15988571 / SRR15988568
*Pma*ES4326ΔDQ3	2,479,212 / 15,275	331.276 / 178.118	31,491	51x / 27x	SRR15988570 / SRR15988567
*Pma*ES4326-C-LA-P5-20-1	1,372,720 / 9,934	189.971 / 146.897	31,020	29x / 22x	TBD / SRR15988569

Table 2: Assembly of *Pma*ES4326 Strains

Strain	Complete Genome	Number of Contigs in Assembly	Replicons Present	Assembly Accession
*Pma*ES4326-D	Yes	5	Chromosome (circular), pPmaES4326ABEF	GCA_000145845.2
*Pma*ES4326-C	No	7	Chromosome (not circular),pPmaES4326ABCDEF	GCA_020309905.1
*Pma*ES4326ΔDQ3	Yes	6	Chromosome (circular), pPmaES4326ABCF	10.6084/m9.figshare.17064080
*Pma*ES4326-C-LA-P5-20-1	No	7	Chromosome (not circular), pPmaES4326ABCDEF	10.6084/m9.figshare.17064080

Figure 1. Comparison of PmaICE-ABAO and PmaECE-DQ. We aligned nucleotide sequences from the pair of potential ICEs found within the *clpB-hopR* region in strain *Pma*ES4326 against each other, and visualize the results here. The top line of the figure displays overall nucleotide identity between these two ICEs, with green bars representing conserved nucleotides and yellow representing slight to modest divergence. If no colored bars on this top line, the sequences are completely divergent, and we highlight the three potential cargo regions that differ between these ICE elements. Predicted loci for each ICE are shown on the lines immediately below the nucleotide identity comparison. *Pma*ICE-ABAQ is positioned immediately adjacent to *clpB* in the *Pma*ES4326 genome while *Pma*ICE-DQ is positioned immediately adjacent to *hopR* in the same genome. Each predicted locus is represented in the figure in blue, while predicted tRNA loci are represented in magenta. We labelled all identified type III effector loci within these regions as well as *clpB*.
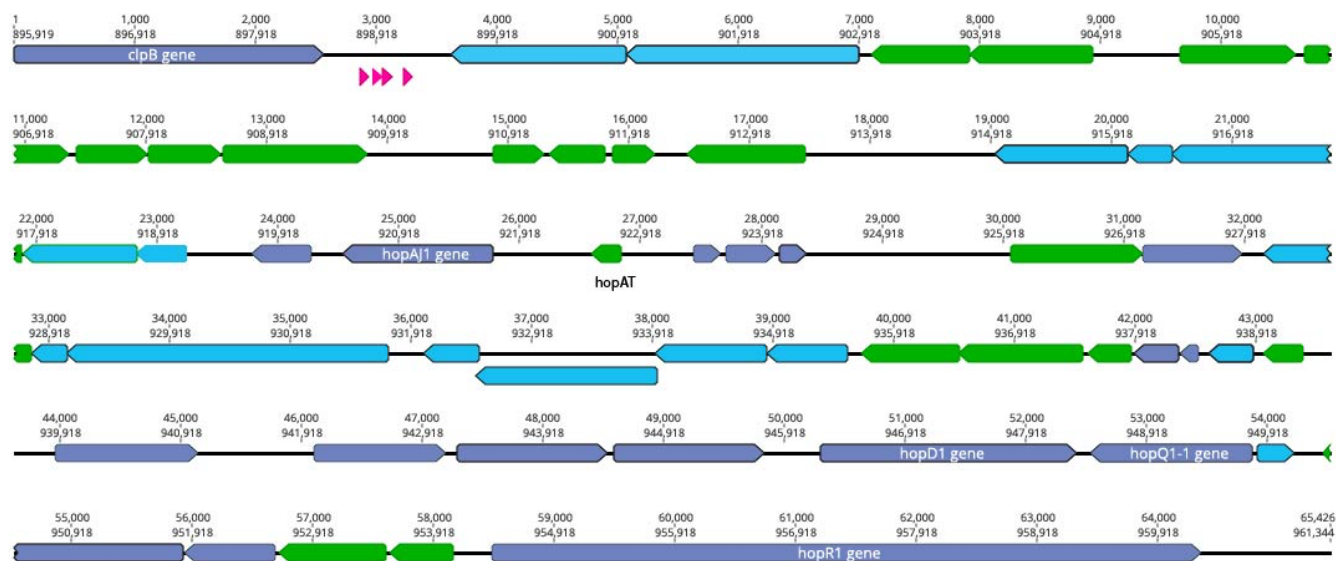
16

533
534

Figure 2. The *clpB-hopR* Region in *Pto*DC3000. Here we visualize the region between *clpB* and *hopR* from the *Pto*DC3000 genome, and compare this region to both predicted ICE elements from *Pma*ES4326. Each predicted locus is colored as purple (present in one of the *Pma*ES4326 ICE elements), blue (present in both *Pma*ES4326 ICE elements as per nucleotide identity), and green (only present in *Pto*DC3000). Predicted tRNA loci are shown in magenta. We also show two nucleotide positions within this region: top number is from the start of *clpB* and the bottom number is from the start of the genome (from *dnaA*). We label all identified type III effector loci as well as *clpB*.

543

544 PmaES4326-C-LA-P5-20-1

545

546 **Figure 3. Identical Deletions of PmaICE-DQ following laboratory selection and passage**

547 **under selective conditions *in planta*.** We compared genomic regions bordering *Pma*ICE-DQ in

548 a strain where the region containing *hopQ* was intentionally deleted (*Pma*ES4326ΔDQ3) as well

549 as a strain that arose after 5 passages *in planta* in *N. benthamiana* (*Pma*ES4326-C-LA-P5-20-1).

550 Mauve alignments of these regions demonstrate that identical evictions of *Pma*ICE-DQ occurred

551 in each strain.

552

18
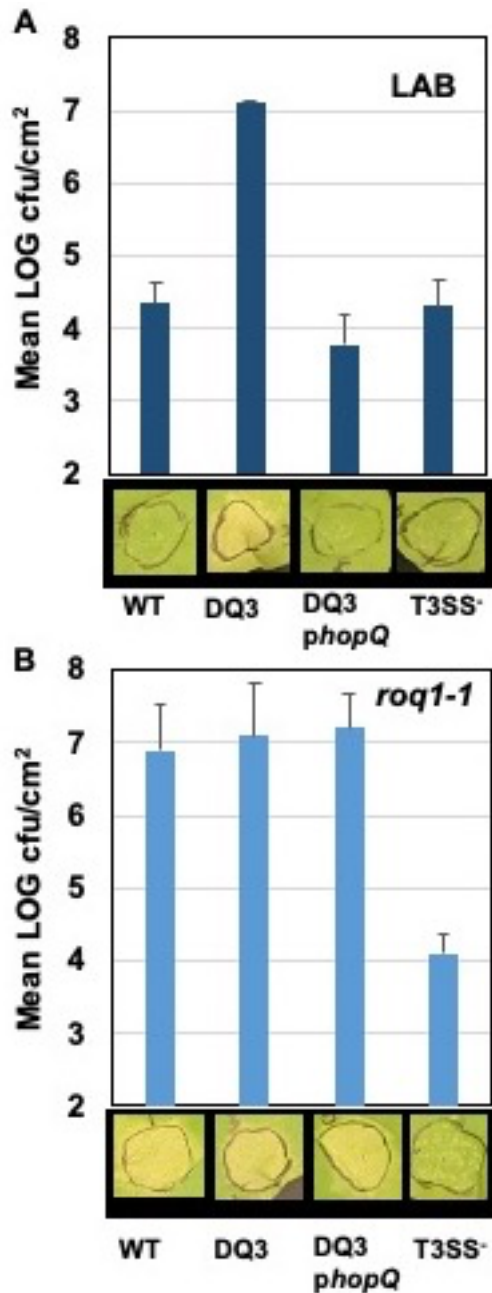
Figure 4. PmaES4326 gains disease compatibility with *N. benthamiana* in the absence of *hopQ/Roq1*-mediated ETI. The PmaES4326 WT strain, ΔDQ3 (ΔPmaICE-DQ), ΔDQ3 complemented with pCPP5372hopQ, and the non-pathogenic T3SS- strain *hrcN*::Tn*5* were infiltrated into leaves of the *N. benthamiana* Lab accession (panel A) or the *roq1-1* CRISPR mutant derivative line (panel B) at 3×10^4 CFU/mL. Eight days post inoculation leaves were photographed to document symptoms and bacterial load from four 4 mm leaf discs from each infiltrated area by dilution plating was determined as CFUs/cm^2 leaf tissue. Values are the means and standard deviations of LOG transformed CFUs/cm^2 from three inoculated plants.
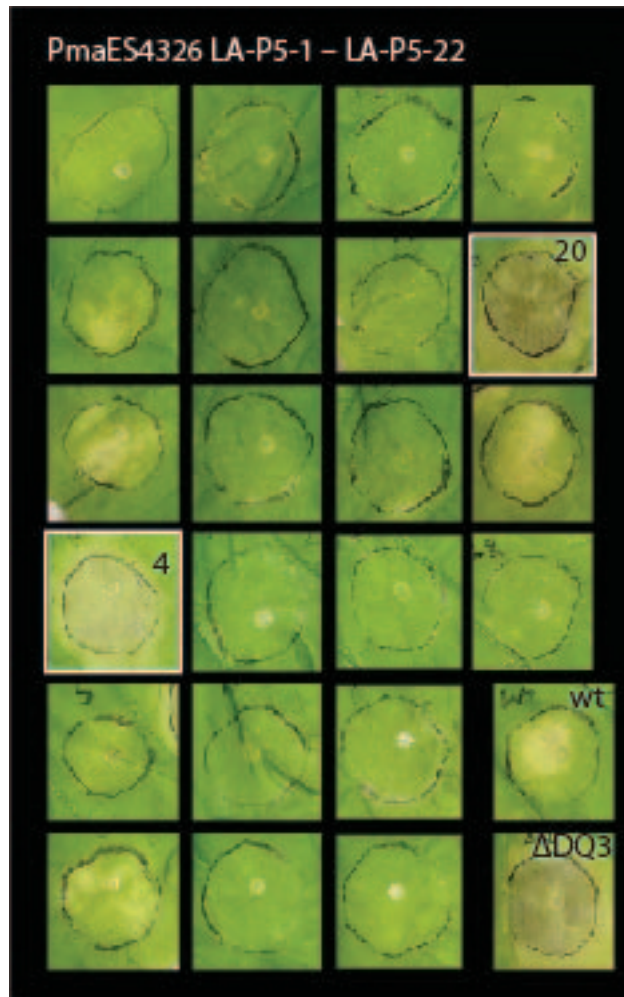
19

Figure 5. A subset of PmaES4326 isolates passaged through *N. benthamiana* gain disease compatibility. Two isolates out of twenty-two *Pma*ES4326 lineage A (LA) passage 5 (P5) isolates produce disease symptoms in the *N. benthamiana* LAB accession comparable to the ΔDQ3 (ΔPmaICE-DQ) strain. Leaves were photographed eight days post inoculation with 3×10^4 CFU/mL bacterial suspensions.
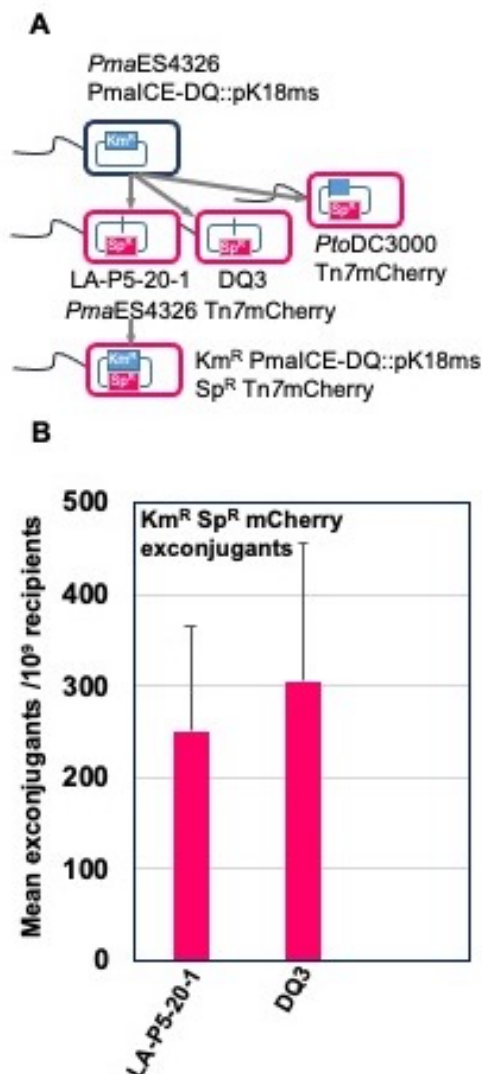
570

Figure 6. PmaICE-DQ can be readily transferred into PmaES4326 strains that lack the ICE
element. (A) Schematic representation of the conjugation strategy for monitoring PmaICE-DQ
transfer between strains. In the donor strain, PmaICE-DQ was marked with kanamycin
resistance by single crossover integration the pK18ms plasmid. The recipient strains
PmaES4326ΔDQ3, PmaES4326-C-LA-P5-20-1 and Pto DC3000 were marked by introduction of a
Spectinomycin resistance Tn73xmCherry marker at their *att*Tn7 sites. Donors and recipients
were co-cultured on LM media and PmaICE-DQ mCherry expressing exconjugants were
recovered on kanamycin and spectinomycin. (B) PmaICE-DQ exconjugant recovery
frequencies/10^9 recipients were determined based on kanamycin and spectinomycin
exconjugants per spectinomycin resistant recipients as determined by dilution plating. Values
are means and standard deviations of three biological replicates.

21

584

585   Adlung, N., Prochaska, H., Thieme, S., Banik, A., Blüher, D., John, P., et al. (2016). Non-host
586   Resistance Induced by the Xanthomonas Effector XopQ Is Widespread within the Genus
587   Nicotiana and Functionally Depends on EDS1. *Front. Plant Sci.* 0.
588   doi:10.3389/fpls.2016.01796.

589   Baltrus, D. A., McCann, H. C., and Guttman, D. S. (2017). Evolution, genomics and
590   epidemiology of Pseudomonas syringae: Challenges in Bacterial Molecular Plant
591   Pathology. *Mol. Plant Pathol.* 18, 152–168.

592   Baltrus, D. A., Nishimura, M. T., Romanchuk, A., Chang, J. H., Mukhtar, M. S., Cherkis, K., et al.
593   (2011). Dynamic evolution of pathogenicity revealed by sequencing and comparative
594   genomics of 19 Pseudomonas syringae isolates. *PLoS Pathog.* 7, e1002132.

595   Bardaji, L., Añorga, M., Echeverría, M., Ramos, C., and Murillo, J. (2019). The toxic guardians
596   — multiple toxin-antitoxin systems provide stability, avoid deletions and maintain virulence
597   genes of Pseudomonas syringae virulence plasmids. *Mob. DNA* 10, 1–17.

598   Baym, M., Kryazhimskiy, S., Lieberman, T. D., Chung, H., Desai, M. M., and Kishony, R. (2015).
599   Inexpensive multiplexed library preparation for megabase-sized genomes. *PLoS One* 10,
600   e0128036.

601   Bolger, A. M., Lohse, M., and Usadel, B. (2014). Trimmomatic: a flexible trimmer for Illumina
602   sequence data. *Bioinformatics* 30, 2114–2120.

603   Botelho, J., and Schulenburg, H. (2021). The Role of Integrative and Conjugative Elements in
604   Antibiotic Resistance Evolution. *Trends in Microbiology* 29, 8–18.

605   Cazorla, F. M., Arrebola, E., Sesma, A., Pérez-García, A., Codina, J. C., Murillo, J., et al.
606   (2002). Copper Resistance in Pseudomonas syringae Strains Isolated from Mango Is
607   Encoded Mainly by Plasmids. *Phytopathology* 92, 909–916.

608   Choi, K. H., Kumar, A., and Schweizer HP (2006). A 10-min method for preparation of highly
609   electrocompetent Pseudomonas aeruginosa cells: application for DNA fragment transfer
610   between chromosomes and plasmid transformation. *J. Microbiol. Methods* 64.
611   doi:10.1016/j.mimet.2005.06.001.

612   Collmer, A., Badel, J. L., Charkowski, A. O., Deng, W.-L., Fouts, D. E., Ramos, A. R., et al.
613   (2000). Pseudomonas syringae Hrp type III secretion system and effector proteins. *Proc.*
614   *Natl. Acad. Sci. U. S. A.* 97, 8770–8777.

615   Colombi, E., Straub, C., Künzel, S., Templeton, M. D., McCann, H. C., and Rainey, P. B. (2017).
616   Evolution of copper resistance in the kiwifruit pathogen Pseudomonas syringae pv.
617   actinidiae through acquisition of integrative conjugative elements and plasmids. *Environ.*
618   *Microbiol.* 19, 819–832.

619   de Vries, S., Stukenbrock, E. H., and Rose, L. E. (2020). Rapid evolution in plant–microbe
620   interactions – an evolutionary genomics perspective. *New Phytol.* 226, 1256–1262.

621   Dillon, M. M., Almeida, R. N. D., Laflamme, B., Martel, A., Weir, B. S., Desveaux, D., et al.
622   (2019a). Molecular Evolution of Pseudomonas syringae Type III Secreted Effector Proteins.

623   *Front. Plant Sci.* 10. doi:10.3389/fpls.2019.00418.

624   Dillon, M. M., Thakur, S., Almeida, R. N. D., Wang, P. W., Weir, B. S., and Guttman, D. S.
625   (2019b). Recombination of ecologically and evolutionarily significant loci maintains genetic
626   cohesion in the Pseudomonas syringae species complex. *Genome Biol.* 20, 1–28.

627   Dong, O. X., and Ronald, P. C. (2019). Genetic Engineering for Disease Resistance in Plants:
628   Recent Progress and Future Perspectives. *Plant Physiol.* 180, 26–38.

629   Godfrey, S. A. C., Lovell, H. C., Mansfield, J. W., Corry, D. S., Jackson, R. W., and Arnold, D. L.
630   (2011). The stealth episome: suppression of gene expression on the excised genomic
631   island PPHGI-1 from Pseudomonas syringae pv. phaseolicola. *PLoS Pathog.* 7, e1002010.

632   Grant, S. R., Fisher, E. J., Chang, J. H., Mole, B. M., and Dangl, J. L. (2006). Subterfuge and
633   manipulation: type III effector proteins of phytopathogenic bacteria. *Annu. Rev. Microbiol.*
634   60, 425–449.

635   Jayaraman, J., Chatterjee, A., Hunter, S., Chen, R., Stroud, E. A., Saei, H., et al. (2021). Rapid
636   Methodologies for Assessing Pseudomonas syringae pv. actinidiae Colonization and
637   Effector-Mediated Hypersensitive Response in Kiwifruit. *Mol. Plant. Microbe. Interact.*
638   doi:10.1094/MPMI-02-21-0043-R.

639   Johnson, C. M., and Grossman, A. D. (2015). Integrative and Conjugative Elements (ICEs):
640   What They Do and How They Work. *Annu. Rev. Genet.* 49. doi:10.1146/annurev-genet-
641   112414-055018.

642   Jones, J. D. G., and Dangl, J. L. (2006). The plant immune system. *Nature* 444, 323–329.

643   Kvitko, B. H., and Collmer, A. (2011). Construction of Pseudomonas syringae pv. tomato
644   DC3000 mutant and polymutant strains. *Methods Mol. Biol.* 712. doi:10.1007/978-1-61737-
645   998-7_10.

646   Kvitko, B. H., Park, D. H., Velásquez, A. C., Wei, C.-F., Russell, A. B., Martin, G. B., et al.
647   (2009). Deletions in the Repertoire of Pseudomonas syringae pv. tomato DC3000 Type III
648   Secretion Effector Genes Reveal Functional Overlap among Effectors. *PLoS Pathog.* 5.
649   doi:10.1371/journal.ppat.1000388.

650   Laflamme, B., Dillon, M. M., Martel, A., Almeida, R. N. D., Desveaux, D., and Guttman, D. S.
651   (2020). The pan-genome effector-triggered immunity landscape of a host-pathogen
652   interaction. *Science* 367, 763–768.

653   LeGault, K. N., Hays, S. G., Angermeyer, A., McKitterick, A. C., Johura, F. T., Sultana, M., et al.
654   (2021). Temporal shifts in antibiotic resistance elements govern phage-pathogen conflicts.
655   *Science* 373. doi:10.1126/science.abg2166.

656   Lovell, H. C., Mansfield, J. W., Godfrey, S. A. C., Jackson, R. W., Hancock, J. T., and Arnold, D.
657   L. (2009). Bacterial Evolution by Genomic Island Transfer Occurs via DNA Transformation
658   In Planta. *Curr. Biol.* 19, 1586–1590.

659   McCann, H. C., Li, L., Liu, Y., Li, D., Pan, H., Zhong, C., et al. (2017). Origin and Evolution of
660   the Kiwifruit Canker Pandemic. *Genome Biol. Evol.* 9, 932.

661   Monteil, C. L., Yahara, K., Studholme, D. J., Mageiros, L., Méric, G., Swingle, B., et al. (2016).

662   Population-genomic insights into emergence, crop adaptation and dissemination of
663   Pseudomonas syringae pathogens. *Microb Genom* 2, e000089.

664   Neale, H. C., Jackson, R. W., Preston, G. M., and Arnold, D. L. (2018). Supercoiling of an
665   excised genomic island represses effector gene expression to prevent activation of host
666   resistance. *Mol. Microbiol.* 110, 444–454.

667   Poulter, R. T. M., Ho, J., Handley, T., Taiaroa, G., and Butler, M. I. (2018). Comparison between
668   complete genomes of an isolate of Pseudomonas syringae pv. actinidiae from Japan and a
669   New Zealand isolate of the pandemic lineage. *Sci. Rep.* 8, 1–13.

670   Qi, D., Dubiella, U., Kim, S. H., Sloss, D. I., Dowen, R. H., Dixon, J. E., et al. (2014).
671   Recognition of the protein kinase AVRPPHB SUSCEPTIBLE1 by the disease resistance
672   protein RESISTANCE TO PSEUDOMONAS SYRINGAE5 is dependent on s-acylation and
673   an exposed loop in AVRPPHB SUSCEPTIBLE1. *Plant Physiol.* 164, 340–351.

674   Qi, T., Seong, K., Thomazella, D. P. T., Kim, J. R., Pham, J., Seo, E., et al. (2018). NRG1
675   functions downstream of EDS1 to regulate TIR-NLR-mediated plant immunity in Nicotiana
676   benthamiana. *Proc. Natl. Acad. Sci. U. S. A.* 115, E10979–E10987.

677   Schierstaedt, J., Bziuk, N., Kuzmanović, N., Blau, K., Smalla, K., and Jechalke, S. (2019). Role
678   of Plasmids in Plant-Bacteria Interactions. *Curr. Issues Mol. Biol.* 30, 17–38.

679   Schultink, A., Qi, T., Lee, A., Steinbrenner, A. D., and Staskawicz, B. (2017). Roq1 mediates
680   recognition of the Xanthomonas and Pseudomonas effector proteins XopQ and HopQ1.
681   *Plant J.* 92. doi:10.1111/tpj.13715.

682   Seemann, T. (2014). Prokka: rapid prokaryotic genome annotation. *Bioinformatics* 30, 2068–
683   2069.

684   Stavrinides, J., and Guttman, D. S. (2004). Nucleotide sequence and evolution of the five-
685   plasmid complement of the phytopathogen Pseudomonas syringae pv. maculicola ES4326.
686   *J. Bacteriol.* 186, 5101–5115.

687   Stavrinides, J., Kirzinger, M. W. B., Beasley, F. C., and Guttman, D. S. (2012). E622, a
688   Miniature, Virulence-Associated Mobile Element. *J. Bacteriol.* 194, 509.

689   Tatusova, T., DiCuccio, M., Badretdin, A., Chetvernin, V., Nawrocki, E. P., Zaslavsky, L., et al.
690   (2016). NCBI prokaryotic genome annotation pipeline. *Nucleic Acids Res.* 44, 6614–6624.

691   Teal, T. K., Lies, D. P., Wold, B. J., and Newman, D. K. (2006). Spatiometabolic Stratification of
692   Shewanella oneidensis Biofilms. *Appl. Environ. Microbiol.* 72, 7324.

693   Wei, C. F., Kvitko, B. H., Shimizu, R., Crabill, E., Alfano, J. R., Lin, N. C., et al. (2007). A
694   Pseudomonas syringae pv. tomato DC3000 mutant lacking the type III effector HopQ1-1 is
695   able to cause disease in the model plant Nicotiana benthamiana. *Plant J.* 51.
696   doi:10.1111/j.1365-313X.2007.03126.x.

697   Wick, R. R., Judd, L. M., Gorrie, C. L., and Holt, K. E. (2017). Unicycler: Resolving bacterial
698   genome assemblies from short and long sequencing reads. *PLoS Comput. Biol.* 13,
699   e1005595.

700